Plasma Phys. Control. Fusion **38** (1996) 1791–1804. Printed in the UK

β_p-collapse-induced vertical displacement event in high β_p tokamak disruption

Y Nakamura†, R Yoshino†, N Pomphrey‡ and S C Jardin‡

† Naka Fusion Research Establishment, Japan Atomic Energy Research Institute, Naka-machi, Naka-gun, Ibaraki 311-01, Japan

‡ Princeton Plasma Physics Laboratory, Princeton University, Princeton, NJ 08543, USA

Received 23 April 1996, in final form 17 June 1996

Abstract. Extremely fast vertical displacement events (VDEs) induced by a strong β_p collapse were found in a vertically elongated ($\kappa \approx 1.5$), high β_p ($\beta_p \approx 1.7$) tokamak with a resistive shell through computer simulations using the tokamak simulation code. Although the plasma current quench which has been shown to be the prime cause of VDEs in a relatively low β_p tokamak ($\beta_p \sim 0.2$) (Nakamura Y *et al* 1996 *Nucl. Fusion* **36** 643), was not observed during the VDE evolution, the observed growth rate of VDEs was almost five times ($\gamma \approx 655\ s^{-1}$) faster than the growth rate of the usual positional instability ($\gamma \approx 149\ s^{-1}$). The essential mechanism of the β_p-collapse-induced VDE was clarified to be the intense enhancement of positional instability due to a large and sudden degradation of the magnetic field decay n-index in addition to the significant destabilization due to a reduction in the stability index n_s. The radial shift of the magnetic axis caused by the β_p collapse induces eddy currents on the resistive shell, and these eddy currents produce a large degradation of the n-index.

It is pointed out that the shell geometry characterizes the VDE dynamics, and that the VDE rate depends strongly both on the magnitude of the β_p collapse and the n-index of the equilibria just before the β_p collapse occurs. The JT-60U vacuum vessel is shown to possess the capability of preventing β_p-collapse-induced VDEs.

1. Introduction

Experimentally observed major disruptions in tokamaks show a rapid plasma current decay (I_p quench) following a β_p collapse, a coincident fast vertical displacement event (VDE) especially in vertically elongated plasmas, and a shrinking plasma boundary [2–4]. A VDE can cause serious wall damage since an unstable plasma with high internal energy can contact plasma-facing components in the vacuum vessel. VDEs have been especially troublesome in machines with non-circular plasma cross sections like JET [5], DIII-D [6], ASDEX Upgrade [7] and JT-60U [4], where the vertically elongated plasma is positionally unstable. It is also well known that a large poloidal halo current with up to 30% of the total plasma current can appear after a large vertical shift in the unstable plasma, and can result in substantial electromagnetic forces acting on structural components [3, 6–9]. The successful operation of next-generation tokamak fusion devices such as ITER [7, 10] will require a detailed understanding of VDE mechanisms and the development of techniques for softening these unfavourable events.

VDE mechanisms for low β_p (≈ 0.2) plasmas in the JT-60U tokamak [1, 11] have been investigated using the Tokamak Simulation Code (TSC) [12]. For these cases, the central electron temperature T_e after the β_p collapse is low, ≈ 100 eV or less [4]. Therefore, an I_p

0741-3335/96/101791+14$19.50

quench immediately follows the β_p collapse, and a fast VDE coincides with the I_p quench. The experimentally observed growth rates of VDEs are at least three times higher than the values predicted by positional stability theory which includes the stabilizing effect of the JT-60U vacuum vessel [1]. Moreover, the experimental evidence indicates a close correlation between the I_p quench rate and the VDE rate. In particular, a rapid I_p quench enhances the VDE rate [4]. TSC computational studies of VDEs showed that the experimentally observed VDE enhancement due to the I_p quench is subject to two major causes [1]. First is the up–down imbalance of attractive forces produced by the eddy current on the JT-60U vacuum vessel, whose shape is slightly asymmetric with respect to the midplane. TSC simulations show a strong dependence of VDE rates on the initial vertical locations of the magnetic axis Z. In particular, plasmas positioned at a neutral location $Z \approx 15$ cm above the midplane prior to the β_p collapse do not exhibit a VDE [11]. VDE avoidance was experimentally established in JT-60U low β_p disruptions [11], as is consistent with the TSC results.

A second cause of VDE enhancement during the I_p quench was found to be the enhancement of the magnetic field curvature, i.e. the degradation of field decay n-index ($n = R/B_Z(\partial B_R/\partial Z) = -R/B_Z(\partial B_Z/\partial R)$), arising from large eddy currents induced by the I_p quench. The n-index degradation leads to an enhancement of the growth rate of positional instability and is especially important in highly elongated tokamaks with $\kappa > 1.7$. In summary, it was clarified that the I_p quench plays a key role in VDE acceleration mechanisms in low β_p tokamaks. In JT-60U disruptive discharges, it was also successfully demonstrated that reducing the impurity influxes during the β_p collapse and the direct neutral beam (NB) heating of the plasma core during the I_p quench are beneficial both for reducing the I_p quench speed and for softening the disruption [2].

The results mentioned above suggest that, unless the plasma current quenches rapidly, fast VDEs do not occur. Therefore, a slow VDE will evolve with a growth rate, which is easy to control utilizing a conventional active feedback system. This statement implies that if the electron temperature T_e after a β_p collapse is high enough to prevent a rapid I_p quench, then the VDE will not occur whatever the value of the plasma β_p prior to the β_p collapse. However, in this paper, we report on a new type of VDE caused by a strong β_p collapse in a high β_p tokamak disruption. In these, an I_p quench does not occur, yet a fast VDE is observed.

In the following sections, we describe numerical results on the onset of VDEs induced by a strong β_p collapse and discuss the fundamental mechanism. Throughout our investigations, self-consistent TSC simulations of deformable plasmas were carried out including the stabilizing effect of the resistive shell. In section 2, the TSC simulation model is described and numerical evidence for the new VDE is presented. In section 3, an investigation of VDE mechanisms is carried out. In section 4, β_p-collapse-induced VDEs in the JT-60U tokamak are discussed in detail with special emphasis on the effect of the shell geometry on the VDE acceleration. Finally, our conclusions are given in section 5.

2. TSC simulation in a model tokamak

2.1. TSC model

The TSC code can accurately compute the full nonlinear axisymmetric and deformable plasma motion including all realistic control aspects, such as an active feedback system, resistive conductors, and circuit and power supply dynamics [12]. However, we will focus on the axisymmetric dynamics of toroidal plasmas electromagnetically interacting only with

the resistive shell, because our interest mainly lies in the rapid processes during the β_p collapse and the subsequent VDE whose time scales are faster than the L/R time of the resistive shell. During a VDE evolution, the coupling of the plasma with the poloidal field (PF) coil circuits can be neglected and the PF coils can be assumed to provide only a static magnetic field, i.e. we can neglect both the active feedback and the passive response of the PF coil system.

The inclusion of details of plasma transport including impurity influx and degradation of energy confinement is beyond the scope of the computational work in this paper. The functional forms of the plasma pressure profile and plasma density profile are assumed to remain unchanged during the TSC simulation. These are given by $p(\bar{\Psi}) = p_0\bar{\Psi}^{3/2}$ and $n(\bar{\Psi}) = n_0\bar{\Psi}$, respectively. Here, $\bar{\Psi}(= (\Psi - \Psi_s)/(\Psi_{axis} - \Psi_s))$ is the normalized poloidal flux. In order to introduce a β_p collapse, the magnitude of the plasma pressure is given as a prescribed time dependence.

In this paper, we also neglect the effect of halo currents on the VDE dynamics. This is justified because JT-60U measurements show no evidence of halo currents during the first half-phase of the disruption [8]. Large amounts of halo current appear in the second half-phase of plasma current termination after a large vertical shift in the magnetic axis [8]. The JT-60U observations are consistent with those of DIII-D and JET [6, 9]. Our main interest here lies in the first half-phase of the disruption, consisting of the rapid β_p collapse followed by the fast VDE evolution on a time scale much shorter than the L/R time of the resistive shell. Another reason for neglecting the halo current in the present study is that here we are interested in mechanisms which accelerate the VDEs, whereas halo currents mitigate the VDEs. A study of the effect of halo current on VDE dynamics is planned as future work.

To investigate the vertical stability in detail, a vertically elongated, bottom-diverted, single-null (SN) tokamak similar to JT-60U and ITER was considered as a model tokamak. Figure 1 illustrates the TSC conductors which model the PF coil system (represented by open boxes) and the resistive shell (represented by closed boxes). The PF coil system is identical to that in the JT-60U. The resistive shell has an up–down symmetry with respect to the mid-plane and is discretized into 34 axisymmetric elements. The inside section of the resistive shell stabilizes the radial shift of the plasma due to the β_p collapse, and the outside sections passively stabilize the vertical plasma displacement. The shell geometry is typical of those commonly used in computational studies on controlling the positional instability in tokamaks [13]. The dominant up–down antisymmetric current mode of the resistive shell, which stabilizes a vertical displacement, has a decay time constant of about 18 ms, while the time constant of the eddy current mode which stabilizes the radial expansion of the plasma was estimated to be about 25 ms. The computational domain is the square box spanning 1.5 to 5.5 m in the major radius direction and -2.0 to 2.0 m in the vertical direction. This domain was divided into (80×80) grids with equal spacing of 5 cm. For reasons of computational efficiency [12], the TSC Alfven time was slowed down by choosing a mass enhancement factor of 50.0. It was verified that this artificial enhancement does not affect the results.

Major plasma parameters for the initial equilibrium just before the β_p collapse are the following: plasma current $I_p = 1.5$ MA, toroidal magnetic field $B_t = 3.5$ T, plasma minor radius $a = 0.76$ m, poloidal beta $\beta_p = 1.7$, and the plasma internal inductance $\ell_i = 1.5$. The plasma shape is characterized by the elongation $\kappa = 1.5$, and the triangularity $\delta = 0.14$. The location of the magnetic axis (R, Z) was (3.33 m, 0.0 m). The magnetic field decay n-index produced by the PF coil systems was -1.5 at the magnetic axis. The growth rate of positional instability including the resistive shell effect was calculated to be 149 s^{-1} using the TSC.

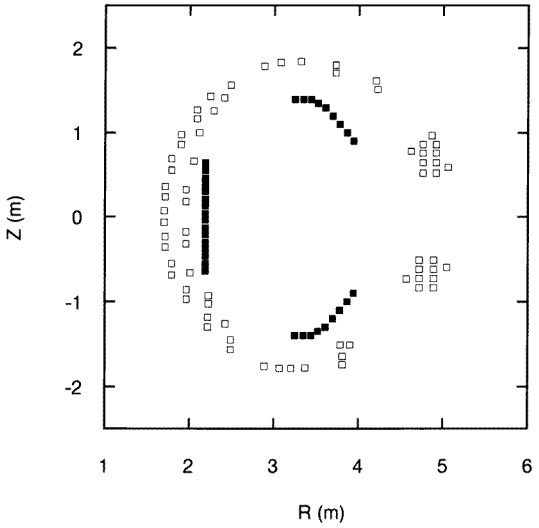

Figure 1. PF coil system (open boxes) and resistive shell (full boxes) of the model tokamak. The computational domain is the square box spanning 1.5 to 5.5 m in the major radius direction and −2.0 to 2.0 m in the vertical direction. This domain is divided into (80×80) grids with equal spacing of 5 cm.

2.2. Extremely fast β_p-collapse-induced VDE

In order to cause a β_p collapse in the high β_p plasma described above, we introduced a rapid plasma pressure drop lasting for 200 μs by assuming a prescribed pressure as a function of the time. Although the time scale of the pressure drop might be considerably faster than the experimental observation of the JT-60U β_p collapse time (a few ms) [2], the rapid pressure drop is a convenient model of the β_p collapse. We can clearly separate the axisymmetric dynamics of high β_p plasma disruptions into a rapid radial shift during the β_p collapse followed by a VDE evolution. In our TSC studies, the β_p collapse is considered to be an initial perturbation given to trigger the VDE. Three magnitudes for the pressure drop defining the β_p collapse were chosen, namely $\Delta\beta_p = -0.5$, -1.0, and -1.5. That is, the β_p values just after β_p collapse were decreased to 1.2, 0.7, and 0.2, respectively. The electron temperature T_e after β_p collapse was assumed to be still sufficiently high (> 3 keV) enough to prevent the VDE-like dynamics caused by the I_p quench.

Figure 2 shows the TSC evolution during the period of 5.0 ms from the onset of the β_p collapse, where the induced eddy current remained nearly constant in time since the L/R time of the resistive shell ($\approx$ 18 ms) is much longer than the period of TSC simulations. Figure 2(a) shows three time-traces of the magnetic axis (R, Z) on a poloidal plane. The β_p collapse lead to coincident radial shifts ΔR of the magnetic axis during the period of 200 μs. The inward shift is due to the mismatch between the vertical field supplied by the PF coils and the required lower vertical field after the plasma pressure drop. The amounts of radial shift, ΔR at 200 μs, were nearly proportional to $\Delta\beta_p$, the severity of the β_p collapse, i.e. $\Delta R = -7.5$ cm for $\Delta\beta_p = -0.5$, $\Delta R = -13.8$ cm for $\Delta\beta_p = -1.0$, and $\Delta R = -21.5$ cm for $\Delta\beta_p = -1.5$. In every case, the β_p collapse provides a small amount of coincident downward displacement of the plasma magnetic axis. The mechanism of the downward perturbation initiating the VDE in bottom-diverted SN tokamaks has been discussed in detail elsewhere [6].

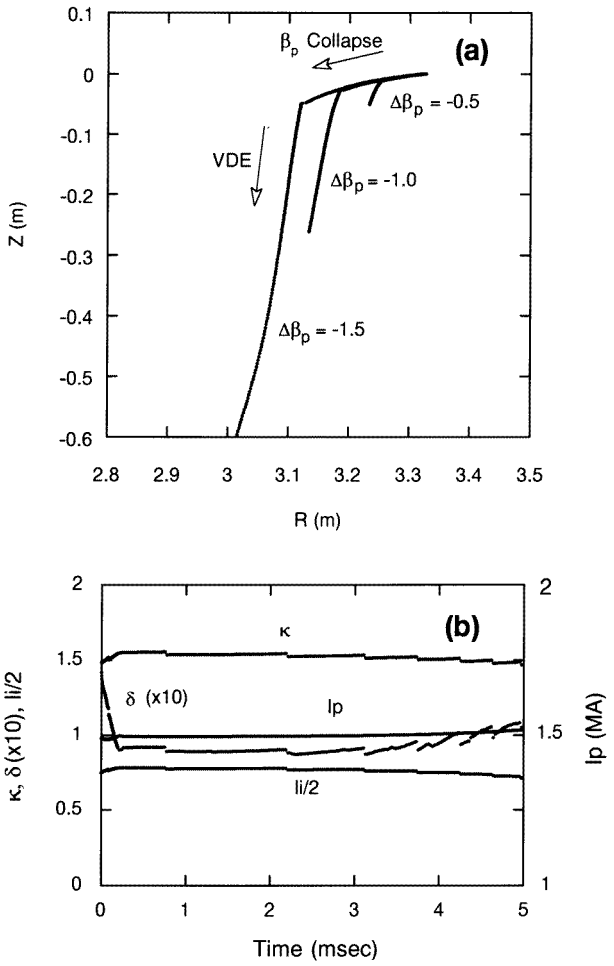

Figure 2. TSC time-evolutions of β_p-collapse-induced VDEs in the model takamak. $\Delta\beta_p$: Severity of β_p collapse of initial plasma ($n = -1.5$) with $I_p = 1.5$ MA, $\beta_p = 1.7$ and $\ell_i = 1.5$. (a) Time-traces of plasma magnetic axis on poloidal plane during 5 ms evolution of β_p-collapse-induced VDE. Extremely fast VDEs were observed for the β_p collapse of $\Delta\beta_p = -1.5$ and -1.0. (b) Time-evolutions of I_p, ℓ_i, κ, and δ for $\Delta\beta_p = -1.0$. The I_p remained nearly constant in time besides the period $t < 200$ μs. The plasma displacement during the VDE evolution was nearly rigid shift until 4 ms, while the δ decreased largely coinciding with the β_p collapse.

Extremely fast VDEs were observed in the cases of β_p collapse with $\Delta\beta_p = -1.5$ and -1.0. For $\Delta\beta_p = -1.5$, a large vertical displacement of $Z = -1.06$ m was obtained 5.0 ms after the β_p collapse. For $\Delta\beta_p = -1.0$, the plasma moved downward to $Z = -26.2$ cm at 5 ms. For $\Delta\beta_p = -0.5$, the vertical position of the magnetic axis remained close to the initial location ($Z = -5.0$ cm at 5.0 ms). Figure 2(b) shows the time evolutions of the plasma current and internal inductance ℓ_i, and the cross sectional shape (characterized by the elongation κ and triangularity δ) for $\Delta\beta_p = -1.0$. The plasma current remained nearly constant in time, although the radial shift due to the β_p collapse led to a small increment in I_p, $\Delta I_p < 0.1$ MA at 200 μs. Both the elongation and the current profile remained constant

until 4 ms after β_p collapse, while the triangularity decreased largely coinciding with the β_p collapse and remained constant after the β_p collapse. This implies that the vertical displacement after the β_p collapse does not accompany both the plasma deformation and the relaxation of current profile until 4 ms, that is, the displacement during the VDE is nearly rigid. For the case of $\Delta\beta_p = -1.5$, the rigid shift was observed during the VDE evolution for a period of 2 ms. For $\Delta\beta_p = -0.5$, the VDE evolved without a deformation for the entire TSC simulation period of 5 ms. The feature of figure 2 we wish to emphasize is that a strong β_p collapse can induce an extremely fast VDE without an I_p quench, and that the VDE can become much faster as the severity of the β_p collapse increases.

The β_p collapse is observed to produce an instantaneous degradation Δn of the vertical field n-index at the magnetic axis. A β_p collapse leads to a radial shift in the plasma which induces a restoring eddy current on the resistive shell. The eddy current on the inside resistive shell flows in the opposite direction to the plasma current, whereas the eddy current on the outside shell flows in the same direction. Consequently, the eddy currents decrease the vertical magnetic field at the plasma and suppress the inward radial shift of the magnetic axis. Such a distribution of eddy currents provides an additional quadrupole moment of the magnetic field in the plasma region, causing the n-index to degrade. The degradation of the n-index persists for the L/R time of the resistive shell.

Figure 3 shows TSC time histories of the n-index and VDE evolutions for the three cases. The n-indices with and without the eddy current effects, as well as the exponential fitting curves of the linear growth of VDEs are shown. At 200 μs, the magnitudes of Δn are -0.3 for $\Delta\beta_p = -0.5$ as is shown in figure 3(a), -0.6 for $\Delta\beta_p = -1.0$ as is shown in figure 3(b), and -1.1 for $\Delta\beta_p = -1.5$ as is shown in figure 3(c), respectively. The small amount of degradation of the n-index neglecting the eddy current effect reflects the fact that the plasma moves inward into a region with a worse equilibrium field n-index. The observed VDE rates were estimated to be 237 s^{-1} for $\Delta\beta_p = -0.5$, 426 s^{-1} for $\Delta\beta_p = -1.0$, and 655 s^{-1} for $\Delta\beta_p = -1.5$, which is almost five times faster than the usual positional instability. It is easy to qualitatively understand why a decrease in the n-index leads to a faster positional instability through the direct application of linear stability theory [14]. However, we will give a more detailed quantitative discussion on the enhancement of VDE caused by the β_p collapse and further investigations of the VDE mechanism in the following section.

3. Mechanism of β_p-collapse-induced VDE

3.1. Degradation of n-index

Figure 4 shows the linear growth rate of positional instabilities as a function of the field decay n-index. The PF coil systems and the resistive shell of the model tokamak utilized in figure 4 are the same as figure 1. The value of n-indices was assigned by introducing an artificial quadrupole field moment, which is constant in time. Major plasma parameters are the same as figures 2 and 3, that is, $I_p = 1.5$ MA and $\ell_i = 1.5$. We consider plasmas with $\beta_p = 1.7$, 1.2, 0.7, and 0.2 as well as the preceding section. To evaluate the growth rates of positional instabilities by TSC simulation, first an initial static equilibrium was obtained after specifying plasma parameters of interest. Next, the plasma was given a small vertical displacement ($Z \approx -1.0$ cm) as an initial condition for the following dynamic simulation, and the TSC time evolution of the vertical displacement was followed during the period of nearly linear growth. The pure exponential growth in the vertical direction was carefully monitored and it was simultaneously verified that the undesirable changes in

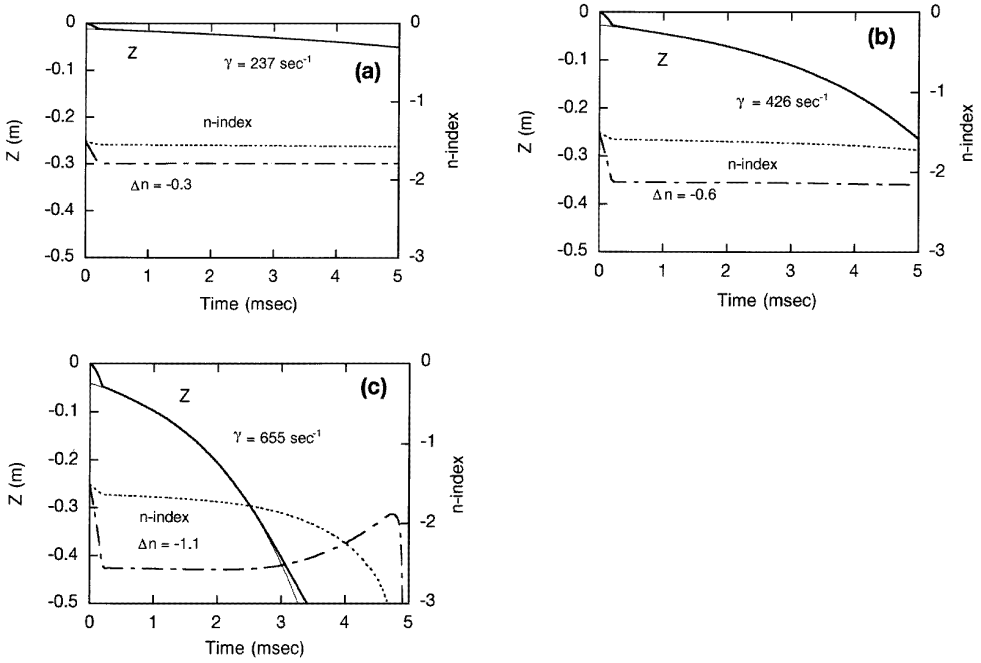

Figure 3. TSC time-evolutions of measured n-index Δn at plasma magnetic axis and VDE dynamics in model tokamak: dotted curve, Δn without eddy current contribution; broken curve, Δn with eddy current contribution. (a) β_p-collapse-induced VDE due to collapse of $\Delta\beta_p = -0.5$. (b) β_p-collapse-induced VDE due to collapse of $\Delta\beta_p = -1.0$. (c) β_p-collapse-induced VDE due to collapse of $\Delta\beta_p = -1.5$.

I_p, β_p, and ℓ_i do not appear during the growth. The initial location R of the magnetic axis for $\beta_p = 1.7$ was 3.33 m, which corresponds to the location prior to the β_p collapse. The R for $\beta_p = 1.2$ was 3.26 m, which corresponds to the radial location just after the β_p collapse of $\Delta\beta_p = -0.5$. The R for $\beta_p = 0.7$ was 3.19 m, and the R for $\beta_p = 0.2$ was 3.11 m, corresponding to the radial locations just after the β_p collapse of $\Delta\beta_p = -1.0$ and -1.5, respectively. All the vertical locations Z were on the midplane ($Z = 0.0$ m).

Figure 4 clearly indicates both that n-index degradation leads to higher growth rates for positional instabilities and that the high β_p plasma is positionally more unstable than the low β_p plasma. We have observed the large degradation of the n-index caused by the β_p collapse as was shown in figure 3. In the case of $\Delta\beta_p = -1.5$, the resultant n-index due to the degradation Δn of -1.1 was -2.6, and the enhanced VDE rate was 655 s^{-1}. Utilizing figure 4, we can obtain a growth rate consistent with the VDE enhancement seen in figure 3(c). Specifically, figure 4 shows that the growth rate of positional instability of the plasma with $\beta_p = 0.2$ and n-index of $n = -2.6$ is $\gamma \approx 670$ s^{-1} at the radial location $R = 3.11$ m. To see this, first follow path (1) along the vertical line of $n = -1.5$ in figure 4, and next, follow path (2) along the curve of the growth rate in the case of $\beta_p = 0.2$. Path (1) corresponds to the β_p collapse of $\Delta\beta_p = -1.5$, and results in an improvement of the positional instability due to the loss of the plasma β_p. The second path (2) corresponds to the enhancement of positional instability due to the degradation $\Delta n = -1.1$. In following path (1), the effect of coincident degradation of n-index provided by the β_p collapse is neglected. The n-index degradation is taken into account only in the second path (2). In the

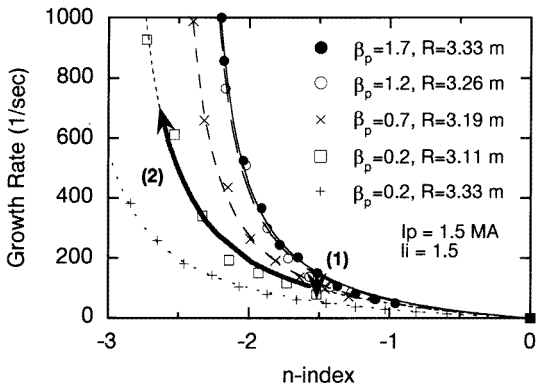

Figure 4. Linear growth rates of positional instabilities against n-index in model tokamak: (1) path corresponding to collapse of $\Delta\beta_p = -1.5$; (2) path corresponding to destabilization of positional instability due to degradation $\Delta n = -1.1$.

cases of $\Delta\beta_p = -0.5$ and -1.0, a similar procedure provides almost the same enhancement of positional instabilities as is shown in figures 3(a) and 3(b), respectively.

3.2. Reduction of stability index

Here, we discuss the effect of the shell geometry on the stabilization of positional instabilities. In particular, we consider how the characteristics of positional instabilities depend on the radial location of the plasmas. According to the linear stability theory using a simple model of rigid shifts of circular-shaped plasmas [14], it is well known that the linear growth rate of positional instabilities is a function of the n-index and the stability index n_s, defined by

$$n + n_s \frac{\gamma \tau_s}{1 + \gamma \tau_s} = 0. \tag{1}$$

Here, τ_s is the effective skin time of the resistive shell. The stability index n_s, which was first defined by Fukuyama *et al* [14], is a useful measure of the positional stability. It is a function of the shell geometry and the plasma parameter $\Lambda (= \ln(8R_p/a) + \beta_p + \ell_i/2 - 3/2)$, i.e.

$$n_s = \frac{2}{\Lambda} \frac{R_p^2}{b^2} \left(1 - \frac{a^2}{b^2}\right)^{-1}. \tag{2}$$

Here, R_p is the plasma major radius, a is the minor radius of the circular plasma, and b is the mean minor radius of the resistive shell. Although equations (1) and (2) cannot express the detailed characteristics of positional instabilities of highly elongated tokamaks with a non-circular-shaped resistive shell as in figure 1, they provide a useful guide to the essential mechanism of positional instabilities considered in this paper. For instance, equations (1) and (2) show that high β_p plasmas are most unstable, and that the inward radial shift of plasmas also results in an increase of the growth rate.

In figure 4, we have presented supplementary TSC results on the linear growth rates of positional instabilities of a plasma with $\beta_p = 0.2$ and $\ell_i = 1.5$. The radial location R was 3.33 m, which corresponds to the location prior to the β_p collapse. The discrepancy between growth rates of the plasmas with the same plasma parameters but located at the

different radial positions of $R = 3.33$ m and $R = 3.11$ m can be seen. Notice that the plasma positioned at the smaller major radius is more unstable than the plasma positioned at the larger major radius. Utilizing equation (2), the stability index n_s of the plasma at $R = 3.11$ m is estimated to be 14% less than the one at $R = 3.33$ m. We obtain a similar reduction of the stability index n_s evaluated from figure 4 by means of a least-squares fit using the form of equation (1), namely, the stability index n_s of the plasma at $R = 3.11$ m is estimated to be 12% less than the one at $R = 3.33$ m. It follows, therefore, that the inward radial shift due to the loss of plasma pressure leads to a reduction of the stability index n_s and results in significant destabilization of positional instabilities.

3.3. Summary

As a consequence of the above considerations, the underlying mechanisms, which characterizes the β_p-collapse-induced VDE in the model tokamak, can be summarized as follows.

(i) The loss of plasma β_p improves the positional instability.

(ii) The inward radial shift of the magnetic axis due to a β_p collapse results in a destabilization owing to the reduction in the stability index n_s.

(iii) The eddy current on a resistive shell induced by the strong β_p collapse degrades the n-index and leads to a significant destabilization.

Mechanisms (ii) and (iii) depend on the specifics of the shell geometry, and will compete with the improvement (i) during disruptions. In the model tokamak, the destabilizing mechanisms (ii) and (iii) overcome the improvement (i), and an extremely fast VDE takes place. Consequently, the optimization of the shell geometry is quite important in order to avoid a β_p-collapse-induced VDE since a variety of resultant VDE characteristics will be seen in elongated tokamaks with a variety of resistive shells. In the next section, we investigate β_p-collapse-induced VDEs of the JT-60U tokamak.

4. β_p-collapse-induced VDEs in the JT-60U tokamak

4.1. TSC simulation

Figure 5 illustrates the TSC configuration of a typical plasma equilibrium and the nominal conductors that model the JT-60U PF coil systems (represented by closed boxes) and the vacuum vessel (represented by open boxes). The dominant up–down antisymmetric current mode of the vacuum vessel has a decay time constant of about 8 ms. The plasma configuration is the same as the high β_p plasma used in section 2, namely, a vertically elongated ($n = -1.5$), bottom-diverted SN plasma with $I_p = 1.5$ MA, $\beta_p = 1.7$, $\ell_i = 1.5$, elongation $\kappa = 1.5$ and triangularity $\delta = 0.14$. The location of the magnetic axis before the β_p collapse is $R = 3.33$ m, $Z = 0.0$ m. The growth rate of positional instability including the shell effect is calculated to be 375 s^{-1} using TSC.

Figure 6 shows TSC time-traces of the magnetic axis on a poloidal plane during the period of 5.0 ms from the onset of the β_p collapse. Three β_p collapses lasting for 200 μs were chosen, namely $\Delta\beta_p = -0.5$, -1.0, and -1.5. The observed inward radial shift ΔR, the degradation of n-index Δn, and the resultant VDE rate γ caused by the β_p collapse are listed in table 1, where those for the model tokamak (see section 2) are also shown. The observed radial shifts ΔR in the magnetic axis after 200 μs are nearly proportional to the severity of the β_p collapse, i.e. $\Delta R = -5.5$ cm for $\Delta\beta_p = -0.5$, $\Delta R = -12.0$ cm for $\Delta\beta_p = -1.0$, and $\Delta R = -18.0$ cm for $\Delta\beta_p = -1.5$. All the plasmas moved downward,

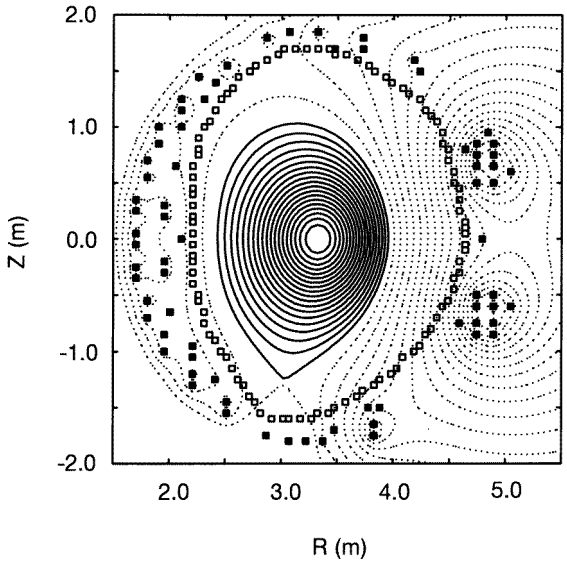

Figure 5. TSC representation of JT-60U plasma equilibrium with PF coil system (full boxes) and vacuum vessel (open boxes).

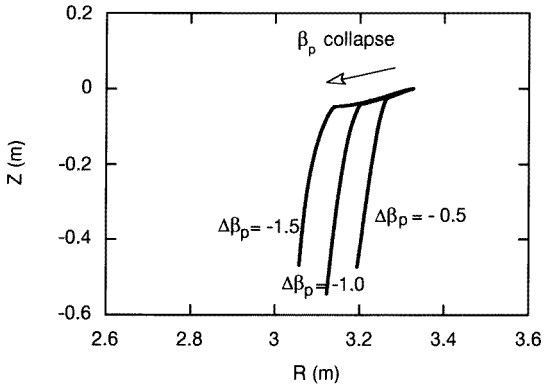

Figure 6. TSC time-traces of plasma magnetic axis on poloidal plane during 5 ms evolution of β_p-collapse-induced VDE in JT-60U tokamak. $\Delta\beta_p$: Severity of β_p collapse of initial plasma ($n = -1.5$) with $I_p = 1.5$ MA, $\beta_p = 1.7$, and $\ell_i = 1.5$.

to around $Z = -50$ cm, 5 ms after the β_p collapse, that is, the VDE dynamics after β_p collapses are similar to each other. During the first 4 ms following the β_p collapse, the total plasma current, plasma shape, and plasma internal inductance remained approximately constant, as observed in the TSC simulations of the model tokamak presented in section 2. Figure 6 implies that a β_p collapse does not accelerate VDEs in the JT-60U tokamak. This contradicts the model tokamak results which show extremely fast VDEs for the case of strong β_p collapse.

The β_p collapse is observed to produce an immediate n-index degradation Δn of the vertical field at the magnetic axis. Figure 7 shows TSC time-histories of the n-index and

Table 1. Comparison of inward radial shift ΔR, degradation of n-index Δn, and resultant VDE rate γ caused by β_p collapse $\Delta\beta_p$.

$\Delta\beta_p$	ΔR (cm) (JT60U/model)	Δn (JT60U/model)	γ (s^{-1})[a] (JT60U/model)
−0.5	−5.5/ − 7.5	−0.2/ − 0.3	345/237
−1.0	−12.0/ − 13.8	−0.4/ − 0.6	316/426
−1.5	−18.0/ − 21.5	−0.6/ − 1.1	264/655

[a] Growth rates of pure positional instability are 375 s^{-1} for the JT-60U and 149 s^{-1} for the model tokamak, respectively.

the VDE evolution in the JT-60U. The n-index degradation remained nearly constant in time for the period of TSC simulations, because the induced eddy current persists during the L/R time of the resistive shell ($\approx$ 8 ms). Table 1 shows that the magnitudes of Δn at 200 μs are −0.2 for $\Delta\beta_p = -0.5$, −0.4 for $\Delta\beta_p = -1.0$, and −0.6 for $\Delta\beta_p = -1.5$, respectively. These Δn values are about half the n-index degradations for the model tokamak. The observed VDE rates were estimated to be 345 s^{-1} for $\Delta\beta_p = -0.5$, 316 s^{-1} for $\Delta\beta_p = -1.0$, and 274 s^{-1} for $\Delta\beta_p = -1.5$. All VDE rates are slower than the pure positional instability (375 s^{-1}). Moreover, as the severity of β_p collapse increases, the VDE growth rate decreases in spite of the observation of the significant n-index degradations. The TSC result contradicts the stability theory [11]. In what follows, we give a more detailed discussion of the β_p-collapse-induced VDE in the JT-60U tokamak.

4.2. Effect of shell geometry

Figure 8 shows the linear growth rate of JT-60U positional instabilities as a function of the decay n-index. Major plasma parameters are $I_p = 1.5$ MA, $\ell_i = 1.5$, and a variety of β_p values (1.7, 1.2, 0.7, and 0.2). The location R of the magnetic axis for $\beta_p = 1.7$ was 3.33 m, which corresponds to the radial location prior to the β_p collapse. The R for $\beta_p = 1.2$ was 3.28 m, the R for $\beta_p = 0.7$ was 3.21 m, and the R for $\beta_p = 0.2$ was 3.15 m, corresponding to the radial locations just after the collapse of $\Delta\beta_p = -0.5$, −1.0, and −1.5, respectively. In each case, the initial vertical locations of the magnetic axis is the midplane position $Z = 0.0$ m. Using figure 8, we can obtain a growth rate consistent with the VDE enhancement for $\Delta\beta_p = -1.5$ seen in figure 7(c), where the resultant n-index due to the degradation Δn of −0.6 was −2.1, and the VDE rate was 274 s^{-1}. By following the paths labelled (1) and (2) in figure 8 as well as the procedure used in section 3, we obtain a growth rate estimate for the β_p-collapse-induced VDE of $\gamma \approx 290$ s^{-1} at the radial location $R = 3.11$ m. In the cases of $\Delta\beta_p = -0.5$ and −1.0, a similar procedure provides almost the same VDE rates as shown in figures 7(a) and 7(b), respectively.

In figure 8, we have presented supplementary TSC results for the linear growth rates of positional instabilities of a plasma with $\beta_p = 0.2$ and $\ell_i = 1.5$. The radial location R is 3.33 m, which corresponds to the location prior to the β_p collapse. Compared with the model tokamak of figure 4, the discrepancy between the growth rates of plasmas positioned at the two different radial locations of $R = 3.33$ m and $R = 3.15$ m is small, implying that the destabilization due to the reduction of stability index n_s is not significant in JT-60U. The stability index n_s of the plasma at $R = 3.15$ m was estimated to be only 5% less than the one at $R = 3.33$ m by means of least-squares fitting using the form of equation (1), while the simple linear stability theory of equation (2) shows that the reduction in the stability index n_s due to a radial shift of 18 cm is about 12%.

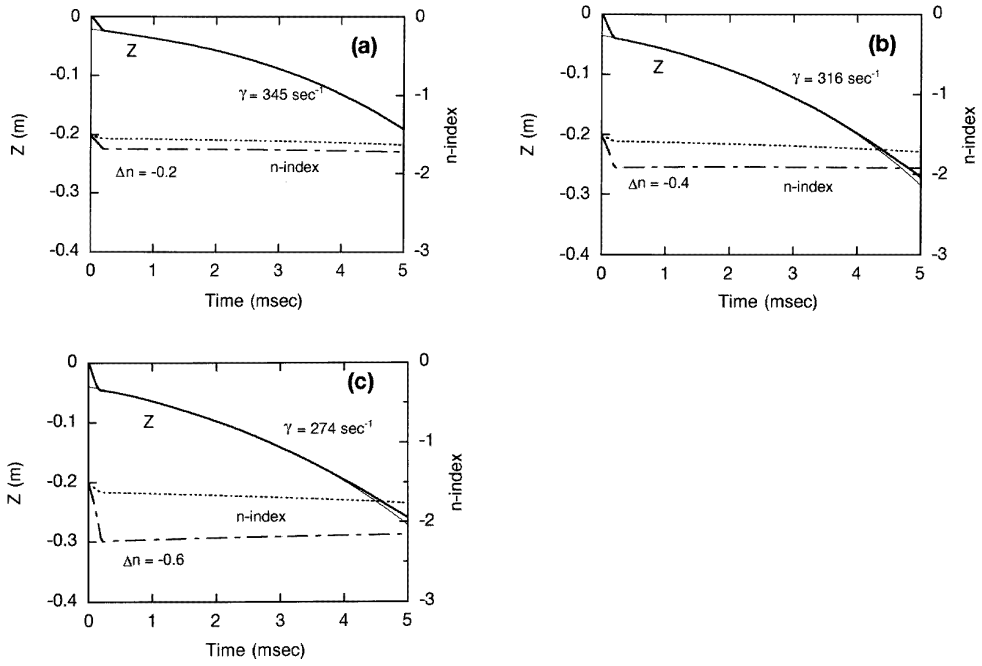

Figure 7. TSC time-evolutions of measured n-index Δn at plasma magnetic axis and VDE dynamics in JT-60U tokamak: dotted curve, Δn without eddy current contribution; broken curve, Δn with eddy current contibution. (a) β_p-collapse-induced VDE due to collapse of $\Delta\beta_p = -0.5$. (b) β_p-collapse-induced VDE due to collapse of $\Delta\beta_p = -1.0$. (c) β_p-collapse-induced VDE due to collapse of $\Delta\beta_p = -1.5$.

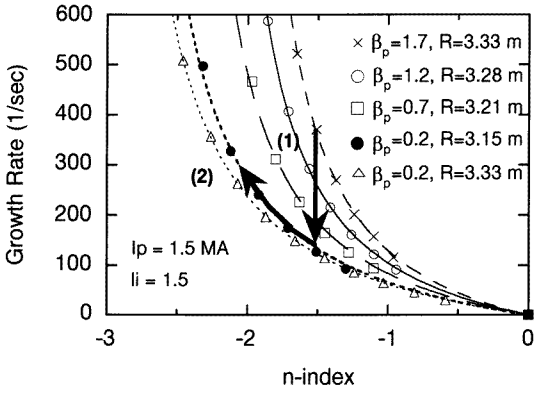

Figure 8. Linear growth rates of JT-60U positional instabilities as a function of n-index: (1) Path corresponding to collapse of $\Delta\beta_p = -1.5$. (2) Path corresponding to destabilization of positional instability due to degradation of $\Delta n = -0.6$.

For the shell geometry of JT-60U, which completely encloses the plasma, the inward radial shift due to a β_p collapse was kept less than -18 cm (as opposed to -22 cm in the model tokamak) and the n-index degradation was ameliorated to be only -0.6 (-1.1 in

the model tokamak). In the JT-60U tokamak, the improvement in the positional instability due to the loss of plasma pressure compensates for the destabilization due to the n-index degradation and the reduction of stability index.

5. Conclusions

In a vertically elongated, high β_p tokamak with a resistive shell, extremely fast VDEs induced by strong β_p collapse were found through computer simulations using TSC. As the magnitude of the β_p collapse increases, the resultant growth rate of the VDE increases. In the case of a strong β_p collapse of $\Delta\beta_p = -1.5$, the VDE rate can be almost five times as fast as the growth rate of the usual positional instability. A plasma current quench, which had been shown to be the prime cause of VDEs in a low β_p tokamak, was assumed not to occur. The essential mechanism of the β_p-collapse-induced VDE was clarified to be the intense enhancement of positional instability due to a large and sudden degradation of the decay n-index in addition to a significant destabilization owing to a reduction of the stability index n_s. The coincident inward radial shift of the magnetic axis due to the decrease in the plasma β_p plays a key role. First, the eddy currents, which are induced by the β_p collapse on the resistive shell to maintain the plasma magnetic axis near the initial location, cause a large degradation of the n-index. Second, the inward radial shift reduces the plasma stability index n_s and leads to a significant destabilization of the positional instability, that is consistent with the linear stability theory.

It was also shown that the shell geometry influences the VDE dynamics, i.e. a variety of VDE characteristics is seen in high β_p tokamak disruptions with a variety of resistive shells. Although extremely fast β_p-collapse-induced VDEs were observed in the model tokamak, severe β_p collapses did not induce VDEs with high growth rates in the TSC studies of the JT-60U tokamak. TSC simulations indicate that the degradation of the n-index remains small; at most $\Delta n = -0.6$ (-1.1 in the model tokamak), and that the reduction of stability index is at worst $\Delta n_s = -5\%$ (-12% in the model tokamak). It follows that the geometry of the JT-60U vacuum vessel, which completely encloses the plasma, possesses the favourable capability of stabilizing β_p-collapse-induced VDEs.

The acceleration mechanism of the β_p-collapse-induced VDE is quite different from that of the I_p-quench-induced VDE. As was discussed in [1], an I_p-quench-induced VDE can be avoided by softening the I_p quench and the optimization of the location of the predisruption equilibrium. However, if a strong β_p collapse of high β_p plasmas occurs, the β_p-collapse-induced VDE will occur even if the I_p quench is absent. The particular nature of MHD activity will determine the speed of the β_p collapse, which is usually very fast compared with the L/R time of a resistive shell in most tokamaks. In such a case, any active feedback would be incapable of preventing the VDE, and a large halo current will be induced on the in-vessel structure after the large vertical shift of the plasma displacement. Therefore, the identification of the β_p-collapse-induced VDE mechanism is important for all elongated tokamaks.

A possible approach to mitigate a β_p-collapse-induced VDE may be the optimization of the shell geometry in order both to keep the inward radial shift of the magnetic axis small and to ameliorate the n-index degradation. In addition, the consequences of a VDE in a mildly elongated tokamak will always be more benign than those in a highly elongated tokamak, therefore the careful selection of the allowable plasma elongation is crucial issue in designing tokamak reactors like ITER. The acceleration mechanism of β_p-collapse-induced VDEs in ITER is now under investigation. Detailed results will be reported together with the generalized design criteria for the VDE-free tokamak in the near future.

Acknowledgments

The authors would like to express their gratitude to Drs M Sugihara and G Kurita for their fruitful comments on the physical meaning of the stability index n_s, and wish to thank Drs M Azumi and T Tsunematsu for their stimulating interest in our work. Dr T Hirayama is also acknowledged for his continuing support.

References

[1] Nakamura Y *et al* 1996 *Nucl. Fusion* **36** 643
[2] Yoshino R *et al* 1993 *Nucl. Fusion* **33** 1599
[3] Sayer R O *et al* 1993 *Nucl. Fusion* **33** 969
[4] Yoshino R *et al* 1995 *Proc. 15th Int. Conf. Plasma Physics and Controlled Nuclear Fusion Research* vol 1 (Vienna: IAEA) p 685
[5] Thomas P R *et al* 1985 *Proc. 10th Int. Conf. Plasma Pysics and Controlled Nuclear Fusion Research* vol 1 (Vienna: IAEA) p 353
[6] Kellman A G *et al* 1991 *Proc. 16th Symp. on Fusion Technology* vol 2 (Amsterdam: Elsevier) p 1045
[7] Gruber O *et al* 1993 *Plasma Phys. Control. Fusion* **34** B191
[8] Neyatani Y, Yoshino R and Ando T 1995 *Fusion Technol.* **28** 1634
[9] Pick M A *et al* 1992 *Proc. 14th Symp. Fusion Engineering* vol 1 (Vienna: IEEE) p 187
[10] Rebut P-H *et al* 1994 The ITER EDA outline design *15th Int. Conf. Plasma Physics and Controlled Nuclear Fusion Research (Seville)* IAEA-CN-60/E-1-I-1
[11] Yoshino R *et al* 1996 *Nucl. Fusion* **36** 295
[12] Jardin S C, Pomphrey N and Delucia J 1986 *J. Comput. Phys.* **66** 481
[13] Ward D J 1990 Studies of feedback stabilization of axisymmetric modes in deformable tokamak plasmas *PhD Thesis* Princeton University, Princeton, NJ
[14] Fukuyama A *et al* 1975 *Japan. J. Appl. Phys.* **14** 871